PHYSICAL REVIEW C VOLUME 19, NUMBER 2 FEBRUARY 1979

Interaction of photons with ^{208}Pb and neighboring isotopes at energies below the neutron emission threshold

R.M. Laszewski and P. Axel
Department of Physics, University of Illinois at Urbana-Champaign, Urbana, Illinois 61801
(Received 13 July 1978)

Average elastic photon scattering cross sections were measured for ^{209}Bi, ^{208}Pb, ^{207}Pb, ^{206}Pb, Tl and Hg at excitation energies between 4.5 MeV and the neutron emission threshold, with an energy resolution in the range between 50 and 150 keV. This resolution was sufficient to determine the strengths of most of the strong levels in this energy region for ^{208}Pb; there are concentrations of strength in a few levels near 5.5 and 7 MeV with the sum of $B(E1)\uparrow$ values equal to about 0.84 and 0.65 e^2 fm^2, respectively; each of these two groups of levels corresponds to only about 0.63% of the electric dipole sum rule. In the neighboring isotopes, approximately the same amount of strength is distributed among many more energy levels; although this strength is spread in energy more than it is in ^{208}Pb, it remains relatively localized.

[NUCLEAR REACTIONS Average $\sigma(\gamma,\gamma)$ measured for ^{209}Bi, ^{208}Pb, ^{207}Pb, ^{206}Pb, Tl and Hg; $\theta = 135°$; E_γ between 4.5 MeV and neutron threshold.]

I. INTRODUCTION

This paper reports a systematic survey of the photon interaction cross section below the photoneutron threshold for ^{208}Pb and its neighboring isotopes. Variable energy photons, with an energy resolution of about 100 keV, were obtained by "tagging" bremsstrahlung photons. This technique had been used in previously reported photon scattering experiments,[1-4] but the larger photon intensity that became available at Illinois made it practical both to study more isotopes over a wider energy range and to improve the statistical accuracy of previous measurements in this part of the periodic table.[3]

Our increased data acquisition rate was made possible by a high duty cycle electron accelerator,[5] MUSL-1, which recirculated an electron beam through a 1.3 GHz superconducting linac that operated with a macroscopic duty cycle of about 50%. The flux of tagged photons on the targets was slightly less than 1 photon/eV sec. We collected data simultaneously in 12 adjacent energy intervals that covered a total energy range of about 1 MeV.

Our 100 keV resolution results complement, and can be interpreted unambiguously due to the availability of, higher resolution elastic scattering studies that used GeLi detectors. For ^{208}Pb, and for its most neighboring isotopes at lower energies, the GeLi experiments have identified the strongest nuclear levels; knowledge of these strong levels makes it possible to correct our poorer resolution, tagged photon measurements for nuclear absorption. For most of the isotopes we have studied, our technique gives a much more reliable estimate of the photon interaction cross sections than can be obtained from the GeLi experiments because the nuclear levels are too closely spaced and too weak to have been observed in survey experiments with GeLi detectors.

The nuclear structure implications of photon scattering are different for ^{208}Pb and for its neighbors. For ^{208}Pb, the properties of levels strongly excited by photons provide important guidance for theoretical calculations which predict the properties of 1^- or 1^+ states that are mixtures of one-particle–one-hole excitations. Below 6.7 MeV in ^{208}Pb, the only 1^- states are believed to be mixtures of one-particle–one-hole states, and these states should therefore be directly comparable with calculations which usually include only one-particle–one-hole excitations. The only multiparticle-multihole 1^- states expected below 7.5 MeV in ^{208}Pb are the two near 6.69 MeV and 6.93 MeV corresponding to the superposition of the 2.61 MeV 3^- state and either the 4.08 MeV 2^+ state or the 4.32 MeV 4^+ state. In the case of 1^+ states, the unperturbed energies of the $h_{11/2}{}^{-1}h_{9/2}$ proton state and the $i_{13/2}{}^{-1}i_{11/2}$ neutron state are 5.57 MeV and 5.85 MeV, respectively. Multiparticle-multihole 1^+ states are expected near 6.08 MeV and 6.67 MeV from combinations of the 2.61 MeV 3^- state, the 3.20 MeV 5^- state and the 3.47 MeV 4^- state.

The nuclear neighbors of ^{208}Pb, in contrast, have many more energy levels of the correct spin and parity to be reached by dipole excitations at energies above 4 MeV. Therefore, a comparison of the photon scattering in the neighboring nuclei to that in ^{208}Pb gives information about the energy region over which the core strength observed in ^{208}Pb is spread in neighboring nuclei. This comparison can also indicate the extent to which the valence nucleons affect the dipole transition strength and its excitation energy.

Most of the photon interaction strength below 7.4 MeV in ^{208}Pb has been identified previously. The strong levels near 6.7 MeV, 7.07 MeV, and 7.33 MeV were first observed with tagged photons[3]; experiments using GeLi detectors provided more accurate values for the energies[6] and resolved the doublet[7] at 7.064 and 7.084 MeV. Similar high resolution experiments also produced the first information[8-10] about photon scattering from levels at 4.84, 5.29, and 5.51 MeV, and from levels near 5.92 and 6.26 MeV. Our new tagged photon data provide reliable values for the relative and absolute scattering cross sections in the entire energy region below 7.4 MeV in ^{208}Pb.

Before we obtained these new data, very little was known about low energy photon interactions cross sections in the neighbors of ^{208}Pb. Earlier tagged photon experiments[3] measured photon scattering cross sections for ^{206}Pb near 7 MeV and for ^{209}Bi near both 5.5 MeV and 7 MeV. Some levels were identified in ^{209}Bi, ^{207}Pb, and ^{206}Pb with the aid of GeLi detectors.[11,12] However, the present moderate resolution experiments determine the elastic scattering cross sections much more reliably particularly for nuclei in which the level spacing is too small to make the identification of individual levels practical.[13,14]

The photon strength functions associated with the ground states of the neighbors of ^{208}Pb are particularly interesting because so much work has been done to determine the photon strength functions of excited states in these nuclei.[15] The data related to excited state strength functions were first cited as evidence for a "pygmy" resonance near 5 MeV; a more recent interpretation was that the strength functions fall abruptly just below 5 MeV but are relatively constant at higher energies.[15] The ground state strength functions which we determine do show a definite concentration in strength near 5.5 MeV for Bi and Pb; for Tl and Hg the strength is represented well by an extrapolation of the giant resonance with modest additional strength near 5.8 MeV; in Tl there is also extra strength near 7.3 MeV.

Our experimental procedure is described in Sec. II and the data analysis is presented in Sec. III. The discussion and conclusions are given in Sec. IV.

II. EXPERIMENTAL PROCEDURE

A simplified diagram of the experiment is given in Fig. 1. The energy, E_β, of an electron beam from the University of Illinois superconducting microtron, MUSL-1, was determined to 0.15% by a combination of slits and a 120° dispersion magnet. Bremsstrahlung produced when the electron beam

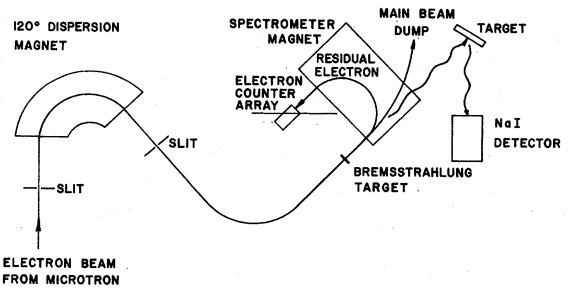

FIG. 1. Simplified diagram of the layout of the experiment.

passed through a thin (20 keV) aluminum foil was collimated to a diameter of 15 cm at the target position. Photons scattered from the target were observed by a 15 cm diameter, 22.5 cm thick NaI detector located at 135° with respect to the direction of the beam. Scattered radiation due to an incident photon of a particular energy, E_γ, was identified with a tagging technique which has been described previously.[1-4] In the present experiment, twelve 5 cm×5 cm×2.5 cm plastic detectors were arrayed contiguously along the focal plane of the spectrometer magnet to detect electrons that had lost energy during the production of γ rays. The energy of residual electrons associated with each of these counters was determined by the field in the spectrometer magnet. A 10 ns coincidence between scattered photons detected in the NaI and a signal from a counter corresponding to a residual electron of energy, E_e, served to determine the energy of the photon that produced the scattering, $E_\gamma = E_\beta - E_e - \Delta$, where Δ is the mean energy loss associated with the ionization caused by an electron passing through the bremsstrahlung foil. Twelve pulse height spectra associated with such coincidences were accumulated simultaneously using an on-line PDP 15 computer. In addition, "chance coincidence" spectra of scattered photons, delayed by an extra 150 ns with respect to the electron counters, were accumulated as a measure of the contribution of accidentals to the coincident spectra. "True coincidence" spectra were obtained by subtracting the corresponding accidentals from the observed coincidences.

At the start of each run the target was removed and the NaI detector was placed directly in a reduced intensity bremsstrahlung beam. In this way, both the photon flux and the response of the NaI crystal to the monoenergetic photons associated with each electron counter were determined. The number of elastically scattered photons was obtained by fitting each "true" spectrum with the measured response function. As an example, Fig. 2(b) shows the response curve of the NaI detector

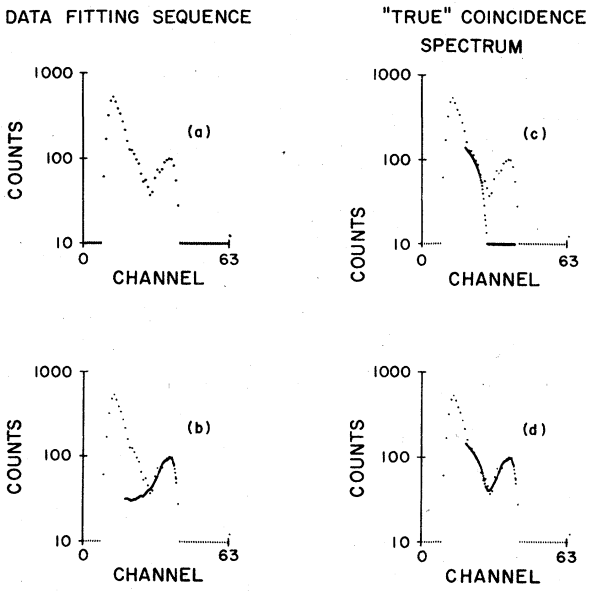

FIG. 2. Data fitting procedure, ^{208}Pb, 7.28 MeV. (a) "True" spectrum: coincidence spectrum minus the corresponding accidentals. (b) The "True" spectrum fit with the detector's measured response function for 7.28 MeV photons. (c) Straight line extrapolation of low energy events. (d) The final fit.

at an energy of 7.28 MeV superimposed on the corresponding ^{208}Pb true coincidence spectrum. The final fit, including an arbitrary straight line extrapolation of lower energy events [Fig. 2(c)] attributable to a combination of atomic and inelastic nuclear scattering from the target, is given in Fig. 2(d).

Our tagged photons have a spread in energy caused mainly by the 2.5 cm width of each electron counter which corresponds to a 2.5% spread in the residual electron energy. Because the energy of the electron beam from MUSL-1 was conveniently variable only in steps of about 3.1 MeV, the resolution of this experiment ranged between about 50 keV and 150 keV.

The incident electron current that could be used during a scattering run was reduced to nanoamperes to decrease "multiple coincidences", i.e., simultaneous coincidences between the NaI detector and more than one electron counter in the array. Macroscopic electron rates were of the order of 5×10^5 electrons/counter second, which corresponds to a tagged photon flux, on target, of about 5×10^4/counter second. Multiple coincidences were 10–20% of the total coincidences. During runs in which the response function was measured by placing the NaI detector directly in the photon beam, pileup limited the total permissible photon flux to much lower values. During these runs, the untagged photon flux of 10^6–10^7 γ/s (E_γ >0.5 MeV) typically corresponded to between 10 and 100 electrons/counter second, or to a tagged flux of 1 to 10 photons per second for each of the 12 γ-ray energies.

III. DATA ANALYSIS

Elastic photon scattering was measured in the energy range from neutron emission threshold down to about 4.5 MeV for samples of enriched ^{208}Pb, ^{207}Pb, ^{206}Pb, and natural Bi, Tl, and Hg. The targets, their isotopic composition, and other relevant parameters are listed in Table I.

The quantity determined by the experiment was N_t/N_γ, the ratio of the number of elastically scattered photons detected at 135° to the number of in-

TABLE I. Target parameters.

Target	Isotope	Abundance	(γ,n) threshold (MeV)	n (atoms/b)
Bi	209	100%	7.5	0.0292
$^{208}PbCO_3$	208	72.6%	7.4	0.0110
	207	1.6%	6.7	
	206	25.8%	8.1	
^{207}Pb	207	84.8%	6.7	0.0327
	208	12.6%	7.4	
	206	2.6%	8.1	
^{206}Pb	206	88.3%	8.1	0.0234
	207	9.0%	6.7	
	208	2.7%	7.4	
Tl	205	70.5%	7.5	0.0298
	203	29.5%	7.7	
Hg	196	0.2%	8.8	0.0420
	198	10.0%	8.3	
	199	16.8%	6.6	
	200	23.1%	8.0	
	201	13.2%	6.2	
	202	29.8%	7.8	
	204	6.9%	7.5	

cident photons of energy E_γ, averaged over the resolution, ΔE. This ratio is related to the differential elastic cross section at 135°:

$$\frac{1}{\Delta E}\int_{\Delta E}\frac{d\sigma}{d\Omega}\bigg|_{135^\circ}\left[\frac{1-\exp[-(2\sigma_e+\beta\sigma_a)n]}{2\sigma_e+\beta\sigma_a}\right]dE=\left(\frac{N_t}{N_\gamma}\right)G\,. \tag{1}$$

G is a number that depends only on the geometry of the experiment and the efficiency of the detector. The factor within large square brackets is the effective sample thickness, corrected for photon absorption in the sample; σ_e and σ_a are the cross sections for atomic and nuclear absorption, respectively, and n is the target thickness perpendicular to the beam. The quantity, β, is the fractional abundance of the isotope responsible for the nuclear absorption. Because the nuclear absorption, σ_a, has a complicated energy dependence, it is difficult to extract $d\sigma/d\Omega$ from Eq. (1) unless special simplifying assumptions are justifiable.

In some of the neighbors of ^{208}Pb, where the level density is high, it can be assumed that individual nuclear levels contributing to the scattering in the excitation interval ΔE have small enough natural linewidths so that the Doppler-broadened nuclear self-absorption is negligible. Equation (1) then yields an expression for the average differential cross section in ΔE:

$$\overline{\frac{d\sigma}{d\Omega}}\bigg|_{135^\circ}\equiv\frac{1}{\Delta E}\int_{\Delta E}\frac{d\sigma}{d\Omega}\bigg|_{135^\circ}dE=\left(\frac{N_t}{N_\gamma}\right)GA\,. \tag{2}$$

The effects of atomic absorption are incorporated in A, which is equal to $1/n$ for small absorption.

$$A=\left[\frac{2\sigma_e}{1-e^{-2\sigma_e n}}\right]\,.$$

The further assumption that only dipole transitions contribute makes it possible to infer the average total cross section, $\bar{\sigma}_{\gamma\gamma}$, from the average 135° differential cross section:

$$S\equiv\bar{\sigma}_{\gamma\gamma}\Big/\overline{\frac{d\sigma}{d\Omega}}_{135^\circ}=\begin{cases}(11.17) & J=0\\ (\sim 12.2) & J=\frac{1}{2}\text{ or }\frac{9}{2}\,.\end{cases}$$

In those cases where individual nuclear levels can be resolved, it is possible to correct for nuclear self-absorption by numerically evaluating the integral in Eq. (1). For an isolated level at energy, E_r, having a total width, Γ, and a ground state width, Γ_0, the nuclear absorption cross section can be expressed in terms of Ψ, the Doppler-broadened line shape which depends on E, E_r, and Γ as well as the mass of the target nucleus and the absolute temperature.[16]

$$\sigma_a(E)=\frac{2\pi}{k^2}\,g\,\frac{\Gamma_0}{\Gamma}\,\Psi\equiv\sigma_0\Psi\,. \tag{3}$$

Using Eq. (3) and the relation between the elastic scattering cross section, $\sigma_{\gamma\gamma}$, and the total absorption cross section, σ_a, Eq. (1) can be rewritten as

$$I(g,\Gamma_0,\Gamma)=\left(\frac{N_t}{N_\gamma}\right)SG\Delta E\,, \tag{4}$$

where

$$I(g,\Gamma_0,\Gamma)=\int\frac{\Gamma_0}{\Gamma}\,\sigma_0\Psi\left[\frac{1-\exp[-(2\sigma_e+\beta\sigma_0\Psi)n]}{2\sigma_e+\beta\sigma_0\Psi}\right]dE\,. \tag{5}$$

For a given target, the value of the integral depends only on g, Γ_0, and Γ; therefore, either knowledge of or assumptions about g and the ground state branching ratio make it possible to determine Γ_0 from the measured scattering.

When the average cross section data contain contributions from levels that are not individually resolvable with tagged photons, but yet have a large enough nuclear self-absorption to require correction, the results of high resolution nuclear

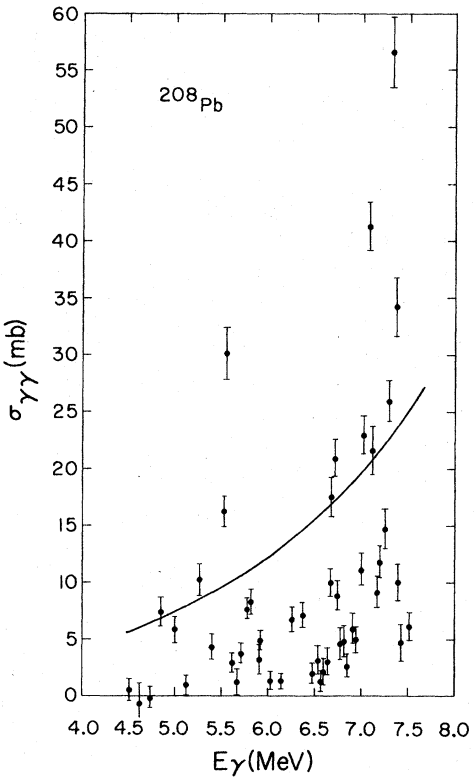

FIG. 3. ^{208}Pb (enriched to 73% 208 isotope): experimental average elastic photon scattering cross sections. The solid curve is a low energy extrapolation of the giant dipole resonance Lorentzian. Note that because the large peaks are dominated by very strong levels, the average "cross section" is governed by the tagged photon resolution; nuclear absorption effects distort the relative intensities.

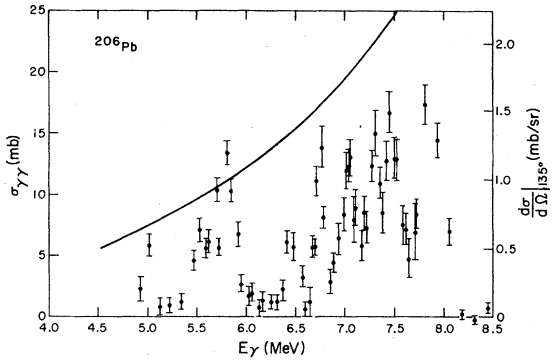

FIG. 4. ^{206}Pb (enriched to 88% 206 isotope): experimental average elastic photon scattering cross sections. The solid curve is a low energy extrapolation of the Lorentz line which fits the giant dipole resonance.

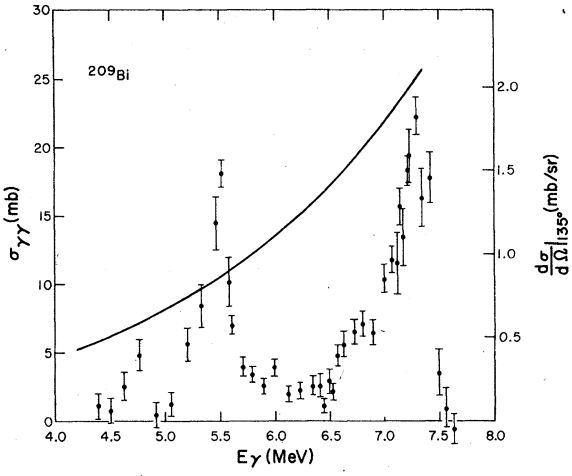

FIG. 6. ^{209}Bi: See Caption of Fig. 4.

resonance fluorescence experiments using GeLi detectors can sometimes be used to determine the appropriate correction to the average measurements. Because experiments with GeLi detectors are most sensitive to the largest levels, the contributions of these levels to the poor resolution, average, cross section can be corrected for self absorption effects.

The experimentally observed average photoelastic cross sections for the three isotopically enriched Pb targets, Bi, Tl, and Hg are presented graphically in Figs. 3–8. These results do not include nuclear self-absorption corrections. The error bars indicate statistical uncertainties only. In calculating the cross sections, we assumed that isotopes in a target did not contribute to elastic scattering at energies above their respective neutron thresholds. In each figure, the Lorentz line extrapolation[15,17,18] of the giant dipole resonance is shown superimposed on the data; the parameters are listed in Table II.

^{208}Pb was the only nucleus among those examined for which the level spacing was large enough so that most strong individual nuclear levels were unambiguously resolved with the tagged photons. This conclusion was reached by comparing our results to those of high resolution GeLi experiments conducted[13,14] at this laboratory. The ground state widths, Γ_0, for the observed levels in ^{208}Pb are listed in Table III. They were obtained by using Eq. (4) to correct for nuclear self-absorption, by assuming that $g=3$ (as it would for dipole scattering from a 0^+ ground state), and that $\Gamma_0/\Gamma=1$. The measured cross sections for the enriched ^{206}Pb and ^{207}Pb targets were used to determine the fraction of the scattering from the enriched ^{208}Pb target that was due to ^{208}Pb. The energies of the lines given in Table III are those determined using GeLi detectors. Table III also gives the transition strengths of the various levels in terms of the reduced transition probability, $B(E1)\uparrow$.

The assumption of negligible nuclear self-absorption that was made in obtaining $\bar{\sigma}_{\gamma\gamma}$ for most targets would be correct if the individual contributing lev-

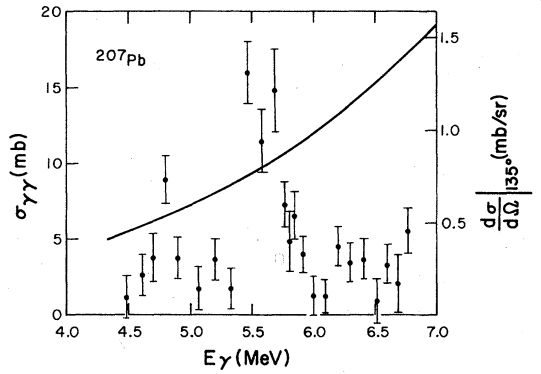

FIG. 5. ^{207}Pb (enriched to 85% 207 isotope): See caption of Fig. 4.

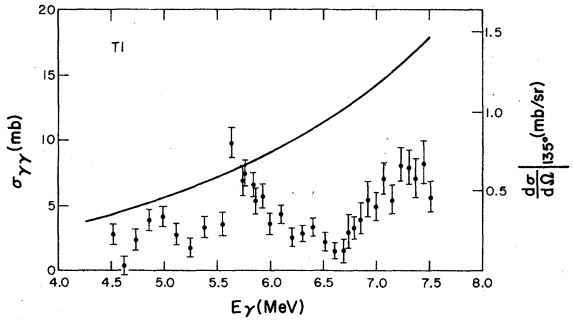

FIG. 7. Natural Tl (71% 205 isotope, 29% 203 isotope): See caption of Fig. 4.

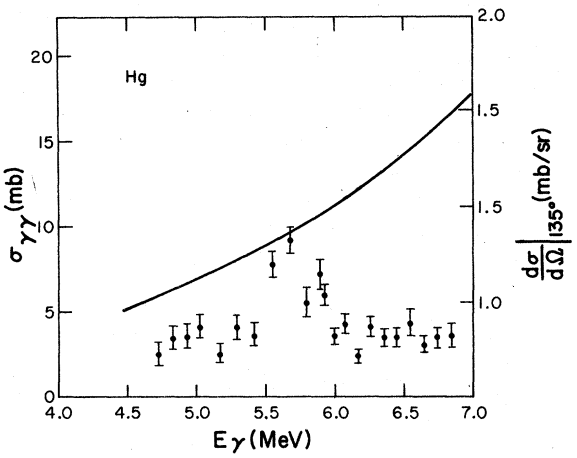

FIG. 8. Natural Hg: See caption of Fig. 4.

els have widths that are less than a few tenths of an eV. Nuclear self-absorption effects would increase the inferred widths of very strong levels, such as those in ^{208}Pb, by almost 30%. Therefore, the average elastic scattering cross sections for the neighbors of ^{208}Pb are a lower limit. They are the actual elastic cross section if the nuclear levels involved have small widths; but if there are very strong levels, the true elastic cross sections will be larger.

The total photon absorption cross section, $\bar{\sigma}_a$, can be deduced from the average elastic cross section, $\bar{\sigma}_{\gamma\gamma}$, if reasonable estimates can be made of the level spacing, D, and the average total width, $\langle\Gamma\rangle$. The total cross section is inferred[4] by assuming that the ground state partial widths, Γ_0, follow a Porter-Thomas distribution, and that the total width, Γ, is related by $\Gamma = \Gamma_0 + \Gamma_c$, where Γ_c is constant. The inferred total cross section for Tl and Hg are given in Figs. 9 and 10. The Lorentz line extrapolations of the giant dipole resonance are again superimposed on the data to simplify comparison of different targets; Table IV summarizes the parameters used to obtain $\bar{\sigma}_a$ from $\bar{\sigma}_{\gamma\gamma}$. Changing either Γ_c or D by a factor of 2 would result in only about a 25% change in the inferred values of $\bar{\sigma}_a$; $\bar{\sigma}_a$ is increased either by increasing Γ_c or by decreasing D.

TABLE II. Giant dipole resonance parameters.

Nucleus	σ_G (mb)	Γ_G (MeV)	E_G (MeV)	Ref.
Bi	521	3.97	13.5	17
^{208}Pb	491	3.90	13.5	17
^{207}Pb	481	3.96	13.6	17
^{206}Pb	514	3.85	13.6	17
Tl	490	3.70	14.1	18
Hg[a]	405	4.5	14.0	15

[a] Values obtained from the sum rule and interpolation.

TABLE III. Nuclear levels in ^{208}Pb (assuming $g\Gamma_0/\Gamma = 3$).

E_γ (MeV)[a]	Γ_0 (eV)	$B(E1)\uparrow$ (e^2 fm^2)
7.332	44.5 ± 2.9	0.322 ± 0.021
7.083, 7.063	25.9 ± 2.1	0.209 ± 0.017
6.721	13.0 ± 1.6	0.122 ± 0.015
5.513	21.4 ± 2.2	0.366 ± 0.038
5.293	7.0 ± 1.4	0.135 ± 0.027
4.842	6.9 ± 1.4	0.174 ± 0.035

[a] References 14, 19–21.

The errors listed for both the calculated cross sections and the ^{208}Pb level widths include only statistical uncertainties. In addition to these statistical uncertainties there is a possible error due to the uncertainty in the photon flux. Experiments indicated that the maximum systematic error in the photon flux could be as large as 8%; however, measurements of the photon flux before and after each scattering run never differed by more than 5%. Uncertainties in the values of the parameters involved in deriving $\bar{\sigma}_{\gamma\gamma}$ and Γ_0 from N_t/N_γ are not large. G is probably known to better than 5%, A to better than 3%, and E to better than 1%. The energy calibration is accurate to between 10 and 20 keV over the entire range of energies examined in this experiment. Thus, the systematic contribution to the error in the tabulated values of the average scattering cross sections, $\bar{\sigma}_{\gamma\gamma}$, is probably not more than about 8%, and the error in the values of Γ_0 is not more than about 10%.

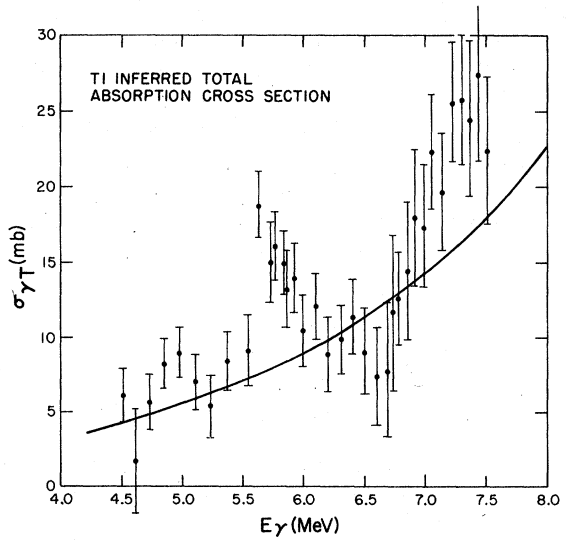

FIG. 9. Tl: inferred total photon absorption cross section.

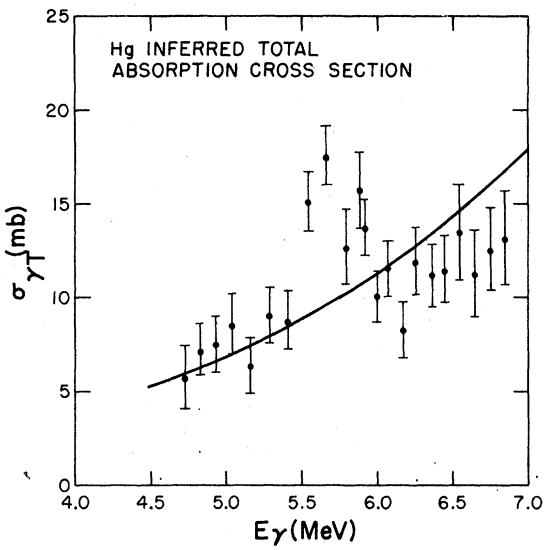

FIG. 10. Hg: inferred total photon absorption cross section.

The nuclear transition matrix element can be obtained from the total photon interaction cross section, $\sigma_{\gamma T}(E)$, integrated over the level of interest. The integrated cross section for a level excited by a γ ray whose energy is $E=\hbar kc=\hbar c/\lambda$ is usually expressed in terms of the ground state width, Γ_0.

$$\int \sigma_{\gamma T} dE = \pi^2 \lambda^2 \left(\frac{2I_e+1}{2I_g+1}\right)\Gamma_0(I_e \to I_g). \tag{6}$$

For a ground state spin $I_g=0$ and for an excited state at $E=7$ MeV with $I_e=1$ and $\Gamma_0=10$ eV, the integrated cross section is 2.35 MeV mb.

The matrix element of interest can be related to the integrated cross section more directly by rewriting Eq. (6) in terms of the reduced transition probability for a dipole transition from the ground state to the excited state. We call this reduced transition probability $B\uparrow$; the more common notation is $B(E1)\uparrow$ and $B(M1)\uparrow$ for electric and magnetic dipole transitions.[24a]

$$\int \sigma_{\gamma T} dE = \pi^2 \lambda^2 \left(\frac{2I_e+1}{2I_g+1}\right)\left(\frac{16\pi}{9}\right) k^3 B\uparrow$$

$$= \frac{16\pi^3}{9} kB\uparrow \tag{7}$$

$$= 0.402E\left(\frac{B\uparrow}{e^2}\right). \tag{8}$$

The reduced electric dipole transition probability dominates over the magnetic dipole transition probability. This dominance is reflected in the conventional units used; $B(E1)$ is usually expressed in units of $e^2\,\mathrm{fm}^2$, which is about 90 times larger than the unit used for $B(M1)$, which is $(e\hbar/2Mc)^2 \equiv \mu_0^2$. Numerically convenient expressions for the integrated cross sections are given in Eqs. (9) and (10),

$$\int \sigma_{\gamma T} dE = 28.1\ \mathrm{MeV\ mb}\left(\frac{E}{7\ \mathrm{MeV}}\right)\frac{B(E1)\uparrow}{e^2\,\mathrm{fm}^2}, \tag{9}$$

$$\int \sigma_{\gamma T} dE = 0.311\ \mathrm{MeV\ mb}\left(\frac{E}{7\ \mathrm{MeV}}\right)\frac{B(M1)\uparrow}{(\mu_0)^2}. \tag{10}$$

The classical $E1$ sum rule can be used to estimate both the sum of $B(E1)\uparrow$ and the total integrated cross section.[24b]

$$\sum_i E_i B_i(E1)\uparrow = 14.8\ \frac{NZ}{A}\ e^2\,\mathrm{fm}^2\,\mathrm{MeV},$$

$$\sum_i E_i B_i(E1)\uparrow = 735\ e^2\,\mathrm{fm}^2\,\mathrm{MeV}\quad \text{for } {}^{208}\mathrm{Pb}. \tag{11}$$

This is equivalent to a total integrated cross section of about 3000 MeV mb; if the average energy of the unperturbed strongly excited one-particle–one-hole states is at 7 MeV, $\sum_i B_i(E1)\uparrow \simeq 105\,e^2\,\mathrm{fm}^2$. The total $M1$ strength expected for ^{208}Pb can be obtained from Bohr and Mottelson's estimate[24c]:

$$\sum_i E_i B_i(M1)\uparrow = 290\ \mathrm{MeV}\mu_0^2 = 3.21\ e^2\,\mathrm{fm}^2\,\mathrm{MeV}. \tag{12}$$

Note that this sum is only about 0.4% of the corresponding electric dipole sum in Eq. (11). This estimate implies a total integrated absorption due to $M1$ which is only 13 MeV mb; if the average energy of the magnetic dipole strength in ^{208}Pb is 8 MeV, $\sum_i B_i(M1)\uparrow = 36\mu_0^2$.

The integrated cross section for $E2$ can be obtained by substituting the appropriate relation between $B(E2)$ and $\Gamma(E2)$ in Eq. (6).

For $E2$,

$$\int \sigma_{\gamma T} dE = \pi^2 \lambda^2 \left(\frac{4\pi}{75}\right) k^5 B(E2)\uparrow$$

$$= 3.10\times 10^{-6} E^3 B(E2)\uparrow\ \mathrm{MeV\ mb}. \tag{13}$$

E is in MeV and $B(E2)$ is in $e^2\,\mathrm{fm}^4$. The classical

TABLE IV. Parameters used in inferring $\bar{\sigma}_{\gamma T}$ from $\bar{\sigma}_{\gamma\gamma}$. (Level spacing is assumed to be of the form $D \propto e^{-E/T}$.)

Nucleus	D_0 (eV)	E_0 (MeV)	T (MeV)	Γ_c (eV)	Ref.
Hg	83	8.03	0.86	0.12	15,22,23
Tl	430	6.54	0.90	0.12	15,22,23

sum rule[24b] can be used to estimate $EB(E2)\uparrow$,

$$\sum_i E_i B_i(E2)\uparrow = \frac{50}{4\pi}\frac{\hbar^2}{2M} Ze^2\langle r^2\rangle , \tag{14}$$

$$\sum_i E_i B_i(E2)\uparrow = 2.05\times 10^5\ e^2\,\mathrm{fm}^4\,\mathrm{MeV} \quad \text{for } ^{208}\mathrm{Pb}.$$

If the fraction (Z/A) of this sum is used to estimate the strength in the isoscalar $E2$ resonance, the corresponding integrated cross section would be 0.25 E^2 MeV mb. Thus, if the isoscalar $E2$ strength is at 10 MeV, as expected, the integrated photon cross section for exciting the resonance would be 25 MeV mb; if the entire isoscalar strength were at 7 MeV, the integrated $E2$ cross section would be only 12 MeV mb.

IV. DISCUSSION AND CONCLUSIONS

A. ^{208}Pb

1. Observed level widths

The level widths we inferred are listed in Table V together with previously reported values. All of the widths in Table V are based on the assumption that the ground state branch of all of the observed levels is 100%. For six of the nine levels listed in Table V (i.e., those at 4.84, 5.29, 5.51, 6.72, 7.06, and 7.08), there is no indication in the higher resolution experiments[13,14] of neighboring weak states. If there are neighboring states that do contribute weakly to elastic scattering, our reported widths include their contribution. A comparison between the relative strengths of the 7.06, 7.08, and 7.33 MeV levels in the GeLi spectra[13,14] and our results indicate that 45 eV of width we report near 7.33 MeV may not all be associated with the one strong level at 7.332 MeV, but may also include contributions from several unidentified neighboring levels. The widths listed in Table V at 5.85 MeV and 6.26 MeV also probably include contributions from more than one level at each energy. Some of the strength we see near 5.85 MeV may correspond to states identified as having $p_{1/2}{}^{-1}d_{3/2}$ neutron configuration from ^{207}Pb(d,p) experiments.[25,9] The 8 eV of ground state width we report near 6.26 MeV probably is associated with more than the 6.262 MeV level reported[14]; we observe somewhat more strength, and other weaker levels were noticed.[14] The peak observed near 6.2 MeV in backward electron scattering would correspond to about 10 eV of ground state width if it were $M1$, but there is no definite evidence on which to base an $M1$ assignment.[26]

2. Comparsion with theory

The interpretation of the photon interaction cross section depends on the multipolarity of the transitions. The amount of strength we see is large enough to make it clear that most of it is $E1$. The integrated cross section centered at 5.5 MeV (i.e., from 5.0 MeV to 6.0 MeV) is 15 MeV mb; there is also about 24 MeV mb between 6.5 MeV and 7.5 MeV. If all of this strength were $E1$, it would correspond to only about 1.3% of the classical sum rule prediction of Eq. (11). Because the pattern of

TABLE V. Comparison of measured level widths.

Energy (MeV)	Γ_0[a] (eV)	Γ_0[b] (eV)	Γ_0[c] (eV)	Γ_0[d] (eV)	I_0 (eV)
4.842	6.9 ± 1.4	6.3	5.7		5.1[e]
5.293	7.0 ± 1.4	8.6	6.8		
5.513	21.4 ± 2.2	28	18		
5.85	4.4 ± 1.1[i]		5.6[j]		
6.262	8.9 ± 1.1[i]	4.1			
6.721	13.0 ± 1.6	15	13	14 ± 7	
7.063	25.9 ± 2.1	29	24	30 ± 13	31[g], 18 ± 3[f]
7.083		14	15		17[g], 16[h]
7.332	44.5 ± 2.9[i]	38	42	41 ± 10	

[a] This work.
[b] Reference 14.
[c] Reference 19.
[d] Reference 3.
[e] Reference 10.
[f] Reference 21.
[g] Reference 11.
[h] Reference 20.
[i] Possibly contains the strength of neighboring weaker levels.
[j] Reported in Ref. 19 for a level at 5.919 MeV.

strength would not change if one or two levels were reassigned as $M1$ or $E2$, our data could serve as a guide to $E1$ strength even if no definite spin-parity assignments were available.

In contrast, almost any of the levels we see would be an important part of either the magnetic dipole or electric quadrupole giant resonance. Inasmuch as the $E2$ isoscalar giant resonance is expected near 10 MeV, and considering that the entire giant would contribute only 12 MeV mb if it were at 7 MeV, it would be surprising indeed if any of the levels were other than dipole. We obtained enough data at 90° to be sure that none of the strong levels is quadrupole. Because the ratio of 90° to 135° scattering is $\frac{2}{3}$ for dipole and 2 for quadrupole, the relative intensity of a quadrupole level would appear three times larger at 90° than at 135°, and this change would have been apparent in our data if any of the strong levels were not excited by dipole excitation.

There have been interesting reports about the giant magnetic dipole resonance in ^{208}Pb. Freedman *et al.*[27] reported a possible 1^+ assignment for the 7.064 MeV level. Using the strength we find for the 7.06–7.08 MeV doublet, and a value of 2 for the ratio of the 7.06 to 7.08 MeV strength,[14] we assign for the 7.06 MeV line a width $\Gamma_0 = 17$ eV which corresponds to $B(M1)\uparrow = 12.7\mu_0^2$. This is equivalent to an integrated cross section of 3.9 MeV mb, which is 30% of the estimated magnetic dipole sum in Eq. (12). Much of the remaining expected $M1$ strength may be located above the neutron threshold.[28,29,30]

In the discussion to follow, we shall assume that all the strength we observe below 7.4 MeV in ^{208}Pb is $E1$. Definite $E1$ assignments have been made[27,31] for the levels at 4.84, 5.29, 5.51, 6.26, 6.72, and 7.08 MeV from measured hadronic inelastic scattering in coincidence with ground state decay γ rays; the levels near 5.85 MeV and 7.33 MeV were not seen in those experiments.

The theoretical implications of the $E1$ strength we observe at low energy are not clear. Previous calculations have concentrated mainly on obtaining a satisfactory description of the energy and strength of the giant $E1$ resonance. These calculations start with zero-order pure one-particle–one-hole states which have about two orders of magnitude more strength at low energy than we observe. The introduction of the particle-hole interaction shifts most of the strength to energies near the observed giant resonance, but leaves a small fraction of the strength at low energy. The results of three calculations of ^{208}Pb for which we have the wave functions and $B(E1)\uparrow$ values are shown in Fig. 11. The larger residual strength at low energy in the earlier calculations[32,33] may be associated with the fact that only Harvey and Khanna[34] properly

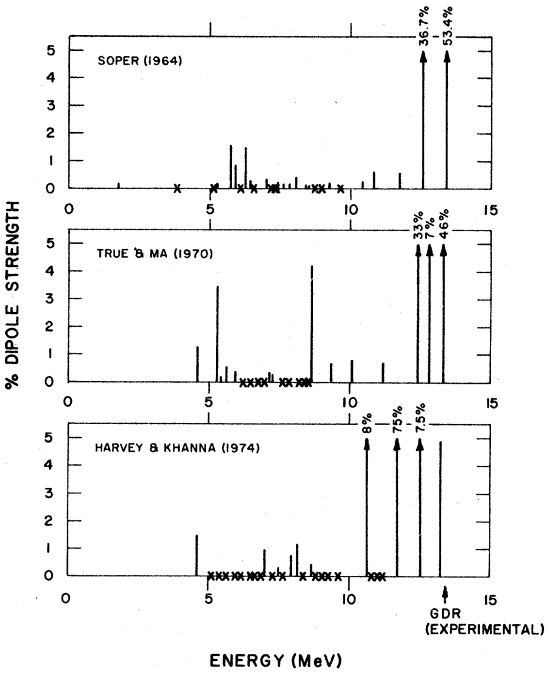

FIG. 11. Comparison of the results of three calculations of the distribution of dipole strength in ^{208}Pb. The arrow indicates the energy at which the giant dipole resonance is observed experimentally.

projected out the spurious state corresponding to the motion of the center of mass. Harvey and Khanna's preferred calculation predicts the lowest 1^- state at 4.49 MeV with a $B(E1)\uparrow$ of 1.28 e^2 fm^2, seven 1^- states from 5.04 MeV to 6.42 MeV with a combined $B(E1)\uparrow$ of 0.25 e^2 fm^2, and six 1^- states from 6.54 MeV to 7.42 MeV with a combined $B(E1)\uparrow$ of 1.72 e^2 fm^2. Our experimental results in Table V show a combined $B(E1)\uparrow$ of 0.84 e^2 fm^2 from 4.84 MeV to 6.26 MeV with the largest value 0.37 e^2 fm^2 associated with the 5.51 MeV state. The $E1$ states between 6.72 MeV and 7.33 MeV have a combined $B(E1)\uparrow = 0.65$ e^2 fm^2. It remains to be seen whether with our results for the strongest 1^- states in hand, theorists can refine their calculations enough to match the energies and photon strengths of these states.

Our experimental results are in agreement with the prediction[34] that the states with the largest $B(E1)\uparrow$ values are mixtures of many one-particle–one-hole configurations. In the calculations, the states with $B(E1)\uparrow$ values equal to or greater than 0.3 e^2 fm^2 did not have more than 15% probability of any single one-particle–one-hole configuration. Stripping reactions[25,9] and analog state reactions[35] indicate that the 5.29 MeV state has a large

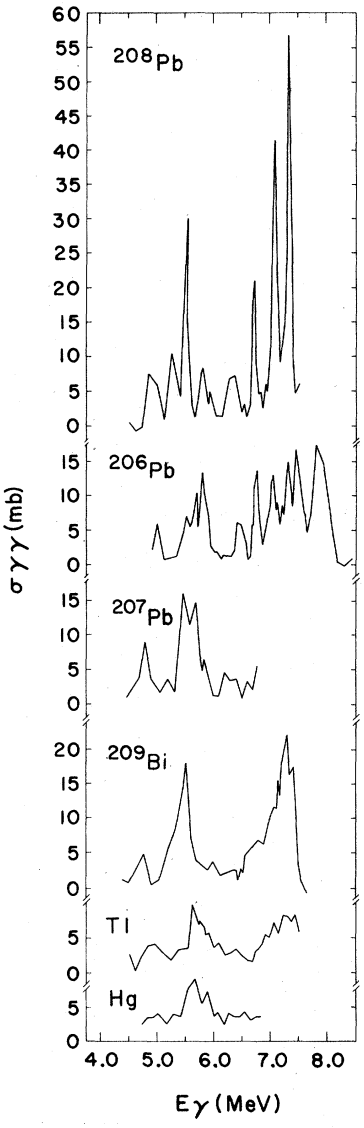

FIG. 12. Comparison of the measured cross sections of, respectively, from the top, ^{208}Pb, ^{206}Pb, ^{207}Pb, ^{209}Bi, Tl, and Hg.

$p_{1/2}{}^{-1}s_{1/2}$ neutron configuration, while states near 5.85 MeV have large $p_{1/2}{}^{-1}d_{3/2}$ neutron strength; our values of $B(E1)\uparrow$ for these levels are only 0.14 e^2 fm^2 and 0.06 e^2 fm^2, respectively.

B. Photon strength in the neighbors of ^{208}Pb

The comparison of the observed elastic scattering cross sections for the Pb isotopes Bi, Tl, and Hg is presented in Fig. 12, and a summary of resolved individual lines from GeLi experiments[13,14] is given in Fig. 13.

The near equality of the photon interaction cross sections of the isotopes that were studied is indi-

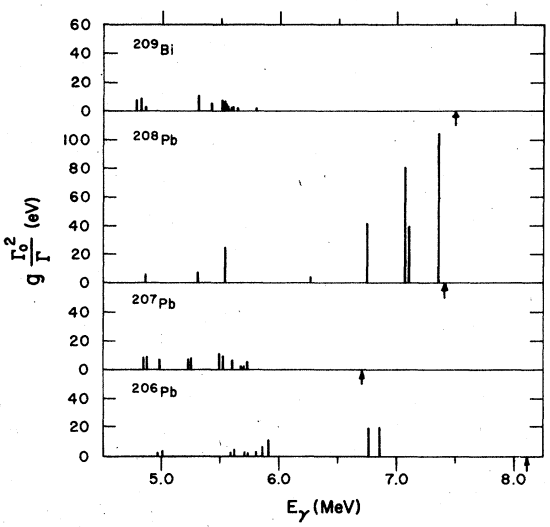

FIG. 13. Summary of resolved individual nuclear lines in ^{209}Bi, ^{208}Pb, ^{207}Pb, and ^{206}Pb from GeLi experiments.[13,14] The arrows indicate the neutron emission thresholds of the respective targets.

cated by the comparison made in Table VI. The values of the integrated scattering cross section, $\int \sigma_{\gamma\gamma} dE$, are compared in two energy regions; the lower energy region is 5.0 to 6.0 MeV, while the upper energy region is 6.5–7.5 MeV. The values given in Table VI are corrected for nuclear absorption, and would be proportional to $B(E1)\uparrow$ if the branching ratio for de-excitation to the ground state, Γ_0/Γ, were 1. All of the variations between isotopes in Table VI might well be explained by the smaller values of Γ_0/Γ expected for the isotopes with larger level density.

The data for the Pb isotopes and Bi strongly suggest that the ^{208}Pb core strength dominates all of these cross sections. The absence of $p_{1/2}$ neutrons in ^{206}Pb and ^{207}Pb appears to shift the strength near 5.5 MeV to slightly higher energy, but the total strength below 6.3 MeV is not much changed. In ^{209}Bi the low energy strength is centered at 5.5 MeV with a full width at half maximum of about 250 keV. Above 6.7 MeV, the ^{206}Pb cross section is consistent with the ^{208}Pb core strength being spread by only about 100 keV; this core strength is not shifted in energy by more than 50 keV unless the 7.45 MeV peak in ^{206}Pb is related to the ^{208}Pb strength at 7.33 MeV. [The energy in MeV of strongest levels in ^{208}Pb up to an energy of 8 MeV, with the ground state widths in parentheses,[36] are 7.41 (5 eV), 7.55, (9.9 eV), 7.62 (16.4 eV), 7.68 (10.2 eV), 7.91 (12.4 eV), 7.98 (19.7 eV), and 8.02 (11.8 eV).] The concentration of strength between 6.7 MeV and 7.4 MeV is also clearly evident in ^{209}Bi, but no substructure is evident; the pattern is consistent with a spreading width of about 500

TABLE VI. Transition strength comparison at 5.5 and 7 MeV.

Nucleus	5.0–6.0 MeV $\int\sigma_{\gamma\gamma}dE$ (MeV mb)	5.0–6.0 MeV %^{208}Pb strength	6.5–7.5 MeV $\int\sigma_{\gamma\gamma}dE$ (MeV mb)	6.5–7.5 MeV %^{208}Pb strength
Bi	10.4	68%	10.7	44%
^{208}Pb	15.2	100%	24.4	100%
^{207}Pb	12.6	83%	...	...
^{206}Pb	15.8	104%	20.2	83%
Tl	8.3	55%	7.8	32%
Hg	11.6	76%	...	...

keV superimposed on the ^{208}Pb core strength.

Indications of some concentrated strength are also evident in Tl (near 5.8 MeV and 7.3 MeV) and Hg (near 5.8 MeV), but in these elements which have both neutron and proton holes, the total strength is more evenly distributed. The inferred total reaction cross sections of Tl and Hg shown in Figs. 9 and 10 indicate modest concentrations of strength superimposed on an extrapolation to low energy of the giant dipole resonance. (Because the giant dipole resonance parameters listed in Table II correspond to about the classical sum rule, whereas the consensus of more recent measurements[17] on heavy elements imply about 1.3 times the classical sum, the inferred total cross sections are somewhat below a modern best estimate of the extrapolation of the giant resonance.) The elastic scattering we measured and the total photon interaction cross section we inferred are quite consistent with the corresponding quantities obtained[37] for ^{205}Tl.

Even though the interaction cross section does not increase monotonically with energy, it is useful to cite some values for the strength function, Γ_0/D, to facilitate comparisons with neutron capture γ-ray studies. The extrapolation of the giant resonance shown in Fig. 9 for Tl corresponds to $10^5\Gamma_0/D = 1.4$, 3.3, and 7.0, respectively, for 5.2, 6.2, and 7.2 MeV. The corresponding values for $k_{E_1} \equiv (\Gamma_0/D)/E^3A^{2/3}$ are approximately $10^9 k_{E_1} = 3$, 4, and 5.4. The quantity k_{E_1} would be energy independent if the sum of $B(E1)\uparrow$ strength per unit energy were independent of energy, and k_{E_1} would be independent of A if the $B(E1)\uparrow$ strength at low excitation energy (where neutron capture data are available) were independent of A. As Eq. (11) indicates, the crudest shell model prediction would be for $B(E1)\uparrow$ to increase approximately in proportion to $A^{4/3}$ because the typical particle-hole energy would be proportional to the oscillator spacing which is $40A^{-1/3}$. Because there is no theoretical guidance about what fraction of $B(E1)$ remains at low energy the particle-hole interaction shifts the unperturbed electric dipole strength up to the giant dipole resonance, and because the terms "single-particle estimate" or "Weisskopf estimate" are misused as though they imply that k_{E_1} is a nuclear constant, values of $10^9 k_{E_1}$ equal to 1 or 2 have been quoted frequently in analyses of some neutron cap-

TABLE VII. The average elastic transition strength $(1/\Delta E)\sum g\Gamma_0^2/\Gamma = (k^2/\pi^2)\bar{\sigma}_{\gamma\gamma}$ in eV of strength per 100 keV interval of excitation for the nuclei neighboring ^{208}Pb.

E (MeV)	^{209}Bi	^{207}Pb	^{206}Pb	Tl	Hg
4.5	0.38	0.06		1.46	
4.6	1.40	0.14		0.18	
4.7	2.13	2.13		1.33	1.49
4.8	2.86	5.37		1.84	2.11
4.9	0.22	2.37	1.46	2.34	2.25
5.0	0.78	1.77	3.84	2.64	2.71
5.1	2.35	1.17	0.53	1.88	2.23
5.2	3.92	2.54	0.56	1.25	1.74
5.3	6.22	1.28	0.89	1.86	2.98
5.4	10.3	6.89	2.76	2.47	2.81
5.5	14.4	12.5	4.63	2.77	4.50
5.6	7.37	9.37	4.56	8.08	6.18
5.7	3.56	12.6	8.81	5.87	7.73
5.8	2.96	4.21	11.8	6.44	4.80
5.9	2.28	3.63	6.17	5.20	6.59
6.0	3.63	1.15	1.58	3.32	3.31
6.1	1.86	1.15	1.85	4.14	4.11
6.2	2.17	4.54	1.29	2.47	2.36
6.3	2.62	3.53	1.24	2.93	4.16
6.4	2.40	3.83	6.58	3.59	3.73
6.5	3.12	0.96	6.21	2.38	3.81
6.6	4.93	3.62	2.76	1.66	4.85
6.7	7.61	2.39	13.1	1.75	3.51
6.8	8.46	6.55	13.7	3.89	4.43
6.9	7.82		5.4	6.76	
7.0	13.1		10.7	6.26	
7.1	15.27		10.5	9.24	
7.2	24.9		11.5	11.1	
7.3	30.7		20.9	11.1	
7.4	25.5		12.0	9.98	
7.5	4.99		19.2	8.24	
7.6			11.3		
7.7			10.7		
7.8			27.8		
7.9			23.7		
8.0			18.1		
8.1			12.4		
8.2			0.37		
8.3			0.42		
8.4			0.86		
8.5			1.30		

ture γ-ray data.

The dependence of k_{E_1} on energy and A has important nuclear structure implications which tend to be lost because of the units in which k_{E_1} is usually expressed. The convenient nuclear unit for the reduced electric dipole transition probability is[24a] the Weisskopf unit $B_W(E1)$:

$$B_W(E1) = \frac{(1.2)^2}{4\pi}\left(\frac{9}{16}\right)A^{2/3}\, e^2\,\mathrm{fm}^2$$

$$= 2.26\left(\frac{A}{208}\right)^{2/3} e^2\,\mathrm{fm}^2 . \qquad (15)$$

k_{E_1} is proportional to the number of Weisskopf units per energy. For example, a value of $k_{E_1} = 10^{-9}$ MeV^{-3} corresponds to 1.48×10^{-2} Weisskopf units of $B(E1)\downarrow$ strength per MeV or about 3.34×10^{-2} e^2 fm^2 per MeV. Values of Γ_0/D obtained in neutron capture studies divided by $E^3A^{2/3}$ would be much more informative if the results were quoted in terms of Weisskopf units of $B(E1)\downarrow$ per MeV rather than in terms of k with units of 10^{-9} MeV^{-3}. Many neutron capture data seem to imply 0.015 to 0.030 Weisskopf units of $B(E1)\downarrow$ per MeV, whereas the extrapolation of the giant dipole resonance for Tl, which is compared to our results in Fig. 9, suggest that at 5.2 MeV, 6.2 MeV, and 7 MeV, respectively, the amount of $B(E1)\downarrow$ per MeV is about 0.045, 0.06, and 0.08 Weisskopf units.

The correspondingly popular parameter quoted for magnetic dipole transitions is $k_{M_1} = \Gamma_0/DE^3$. A value of $k_{M_1} = 10^{-9}$ MeV^{-3} corresponds to 4.82×10^{-2} Weisskopf units of $B(M1)\downarrow$ per MeV.

The development and operation of MUSL-1 and its experimental areas was supported by a grant from the National Science Foundation.

APPENDIX

This appendix presents Table VII, which tabulates the average elastic transition strength

$$\frac{1}{\Delta E}\sum g\,\frac{\Gamma_0^2}{\Gamma} = \frac{k^2}{\pi^2}\,\bar{\sigma}_{\gamma\gamma}$$

in eV of strength per 100 keV interval of excitation for the nuclei neighboring ^{208}Pb. The average is listed for uniform increments of the excitation energy to facilitate comparisons among the various nuclei. A Weisskopf unit is about 500 eV at 6 MeV, so that 3 eV/100 keV would be 0.06 Weisskopf units per MeV. The errors to be assigned to these numbers correspond to the errors in $\bar{\sigma}_{\gamma\gamma}$ as discussed in the paper. They are typically 10 to 20% except on the smallest numbers tabulated, for which the errors are no more than about 1.5 eV/100 keV.

[1] J. S. O'Connell, P. A. Tipler, and P. Axel, Phys. Rev. 126, 228(1962).
[2] P. A. Tipler, P. Axel, N. Stein, and D. C. Sutton, Phys. Rev. 129, 2096 (1963).
[3] P. Axel, K. Min, N. Stein, and D. C. Sutton, Phys. Rev. Lett. 10, 299 (1963).
[4] P. Axel, K. K. Min, and D. C. Sutton, Phys. Rev. C 2, 689 (1970).
[5] A. O. Hanson, IEEE Trans. Nucl. Sci. NS-18, 149 (1971); L. M. Young, *ibid.* NS-20, 81 (1973); P. Axel, A. O. Hanson, J. R. Harlan, R. A. Hoffswell, D. Jamnik, D. C. Sutton, and L. M. Young, *ibid.* NS-22, 1176 (1975).
[6] A. M. Khan and J. W. Knowles, Bull. Am. Phys. Soc. 12, 538 (1967).
[7] C. P. Swann, Bull. Am. Phys. Soc. 12, 1066 (1967).
[8] A. M. Khan and J. W. Knowles, quoted in Ref. 9.
[9] E. D. Earle, A. J. Fergusun, G. Van Middlekamp, G. A. Bartholomew, and I. Bergqvist, Phys. Lett. 32B, 471 (1970).
[10] C. P. Swann, Phys. Rev. Lett. 32, 1449 (1974).
[11] C. P. Swann, Nucl. Phys. A201, 534 (1973).
[12] C. P. Swann, J. Franklin Inst. 298, 321 (1974).
[13] D. F. Coope, Ph.D. thesis, University of Illinois, 1975 (unpublished).
[14] D. F. Coope, L. E. Cannell, and M. K. Brussel, Phys. Rev. C 15, 1977 (1977).
[15] G. A. Bartholomew, E. D. Earle, A. J. Ferguson, J. W. Knowles, and M. A. Lone, in *Advances in Nuclear Physics*, edited by M. Baranger and E. Vogt (Plenum, New York, 1973), Vol. 7, p. 229.
[16] E. R. Metzger, Prog. Nucl. Phys. 7, 54 (1959).
[17] B. L. Berman and S. C. Fultz, Rev. Mod. Phys. 47, 713 (1975).
[18] G. P. Antropov, Bull. Acad. Sci. USSR. Phys. 34, 108 (1970).
[19] J. W. Knowles, A. M. Khan, and W. F. Mills (to be published).
[20] W. Scholz, H. Bakhra, R. Colle, and A. Li-Scholz, Phys. Rev. C 9, 1568 (1974).
[21] R. J. Sparks, H. Lancman, and C. Van Der Leun, Nucl. Phys. A259, 13 (1976).
[22] J. E. Lynn, *The Theory of Neutron Resonance Reactions* (Clarendon, Oxford, 1968).
[23] H. Molecky, Sov. J. Nucl. Phys. 13, 133 (1971).
[24] A. Bohr and B. Mottelson, *Nuclear Structure* (Benjamin, New York, 1969), (a) Vol. 1, p. 382, (b) Vol. 2, pp. 403–404, (c) Vol. 2, p. 638.
[25] M. Dost and W. R. Hering, Phys. Lett. 26B, 443 (1968).
[26] L. W. Fagg, private communication.
[27] S. J. Freedman, C. A. Gagliardi, G. T. Garvey, M. A. Oothoudt, and B. Svetitsky, Phys. Rev. Lett. 37, 1606 (1976).
[28] R. J. Holt and H. E. Jackson, Phys. Rev. Lett. 36, 244 (1976).
[29] R. M. Laszewski, R. J. Holt, and H. E. Jackson, Phys. Rev. Lett. 38, 813 (1977).
[30] S. Raman, M. Mizumoto, and R. L. Macklin, Phys. Rev. Lett. 39, 598 (1977).
[31] R. M. Del Vecchio, S. J. Freedman, G. T. Garvey, and M. A. Oothoudt, Phys. Rev. C 13, 2089 (1976).
[32] M. K. Pal, J. M. Soper, and A. P. Stamp, Harwell Report

T. P. 148, 1964 (unpublished).
[33]W. W. True, C. W. Ma, and W. T. Pinkston, Phys. Rev. C 3, 2421 (1971).
[34]H. Harvey and C. F. Khanna, Nucl. Phys. A221, 77 (1974), and private communication.
[35]J. G. Cramer, Phys. Rev. Lett. 21, 297 (1968).
[36]R. E. Toohey and H. E. Jackson, Phys. Rev. C 6, 1440 (1972).
[37]E. D. Earle, J. W. Knowles, M. A. Lone, and G. A. Bartholomew, Nucl. Phys. A257, 365 (1976).